Raman Spectra of Poly(2,3-R,R-thieno[3,4-*b*]pyrazine). A New Low-Band-Gap Polymer

J. Kastner and H. Kuzmany*

Institut für Festkörperphysik, Universität Wien, 1090 Wien, Austria

D. Vegh and M. Landl

Department of Organic Chemistry, Slovak Technical University, Bratislava, Slovakia

L. Cuff and M. Kertesz

Chemistry Department, Georgetown University, Washington, D.C. 20057–2222

Received September 21, 1994; Revised Manuscript Received January 30, 1995[⊗]

ABSTRACT: Vibrational modes of the new processable polymer poly(2,3-R,R-thieno[3,4-*b*]pyrazine) with a band gap of about 0.9 eV were measured by resonance Raman scattering and calculated by a quantum chemical method. Raman spectroscopy of the pristine polymer revealed a strong line at about 1520 cm^{-1} and doublet structure at around 1560 cm^{-1} in the C=C stretching region. By changing the exciting laser line these lines exhibit a dispersion which is about 16 cm^{-1}/eV for the line at 1520 cm^{-1}. Substitution at the 2,3-positions with alkyl groups has only a weak influence on the vibrational properties. Several modes shift moderately toward lower frequencies with increasing chain length. The utilization of thiophene rings as substituents results in a much more efficient mode softening. In addition, the Raman response of $FeCl_3$-doped samples is presented. Changes in relative intensities and weak line shifts were observed. Calculations on the ground state revealed that the quinonoid structure is by about 13 kcal/mol per repeat unit more stable than the aromatic form. By using the scaled quantum mechanical oligomer force field (SQMOFF) method the Raman spectrum of the quinonoid form was calculated. According to this the lines observed experimentally in the C=C stretching mode region originate from the inter-ring A_g vibration and from an A_g mode which mainly comprises intra-ring stretches superposed with a B_{2g} mode. The vibrational results are consistent with the calculated quinonoid ground-state geometry.

I. Introduction

Conjugated polymers with a small energetic separation between occupied and unoccupied bands have attracted considerable attention in connection with attempts to make intrinsic organic metals and new and efficient nonlinear optical materials.[1-9] In addition, they are expected to absorb less visible light in the doped conducting state than in the neutral state and thus provide conducting transparent materials. Several routes to design and synthesize low-band-gap polymers have been reported.[4-9] Bredas et al.[2] have shown that the band gap is more or less proportional to the bond length alternation along the polymeric backbone. The addition of cyclic side groups and the incorporation of alternating organic segments, which tend to drive the backbone into an aromatic and into a quinonoid configuration, are two possible ways to level the bond length alternation and to approach an intrinsic metallic state. Some of these so-called "interchanged bond alternation system" (IBAS) polymers have been already synthesized, and a reduction of the gap was observed.

The first low-band-gap species was poly(isothianaphthene) (PITN),[1] which has a band gap of about 1 eV. From the very beginning of its discovery there has been an intensive discussion concerning the ground state. Bredas et al.[2] suggested an aromatic ground-state geometry with a long inter-ring bond length, whereas Lee and Kertesz[10] calculated a quinonoid geometry to be the energetically favored state for PITN. Especially, the joint experimental and theoretical study on the Raman modes turned out to be a powerful method for the determination of the ground-state geometry.[3,5] Raman spectra of neutral and doped PITN were measured and compared with calculations for the quinonoid and aromatic form. In this way the ground state of PITN was assigned to a quinonoid structure.[3,5] NMR measurements[11] as well as more recent quantum chemical calculations and experimental results[12] support also the quinonoid ground-state geometry.

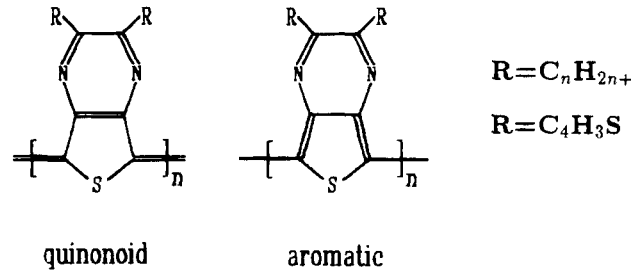

Figure 1. Chemical structure of poly(2,3-R,R-thieno[3,4-*b*]-pyrazine) for the quinonoid and aromatic form.

Recently a new low-band-gap compound poly(2,3-R,R-thieno[3,4-*b*]pyrazine) (PThP) substituted with hexyl groups was synthesized.[8] The chemical structures of both the quinonoid and aromatic forms are shown in Figure 1. Its experimentally observed band gap was about 0.9 eV, making it to one of the lowest band-gap polymers prepared so far. In contrast to PITN this polymer is soluble in common organic solvents and thus easily processable, which makes PThP very attractive for applications. The electronic structure of PThP was predicted by Nayak and Marynick[13] to be essentially the same as that of PITN,[10] namely, quinonoidal in the ground state.

In this paper we present a joint experimental and theoretical study on the vibrational properties of PThP. Raman modes of the pristine and $FeCl_3$-doped polymer

[⊗] Abstract published in *Advance ACS Abstracts,* March 15, 1995.

0024-9297/95/2228-2922$09.00/0

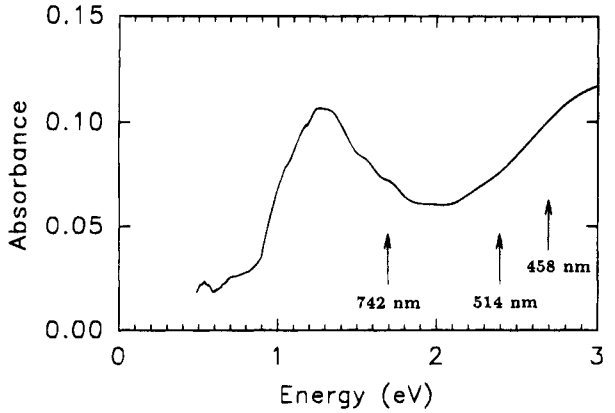

Figure 2. Optical absorption spectrum of a thin film of poly-(2,3-R,R-thieno[3,4-*b*]pyrazine) substituted with R = n-$C_{13}H_{27}$. The arrows mark positions of laser lines used for the excitation of the Raman spectra.

were measured by Raman spectroscopy after excitation with various laser frequencies. The influence of substituents at the 2,3-positions such as alkyl and thiophene groups on the vibrational properties is studied and elucidated. Quantum chemical calculations for both the stabilization energy and the Raman spectra are presented. By comparing theoretical and experimental results, the structure of the ground state is determined to be quinonoid, in agreement with earlier predictions.[13] A tentative assignment of the Raman modes is also given.

II. Experimental Section

The preparation of the monomers 2,3-R,R-thieno[3,4-*b*]-pyrazine with R = C_nH_{2n+1} (n = 1, 2, 6, 11, and 13) and 2-thienyl (thiophene) was published elsewhere.[14] Polymerization was performed in $CHCl_3$ solution for 24 h by the oxidative coupling of the monomers using $FeCl_3$ as oxidant, while dry air was bubbled through the reaction mixture. This yielded the oxidized form which means the doped form of the polymer. Dedoping was performed with concentrated aqueous ammonia. From $CHCl_3$ solution thin films were formed on silicon and glass substrates by casting. Optical absorption was measured using a Hitachi U-3410 spectrophotometer. The optical absorption in the Vis–near-IR spectral range of an undoped poly(2,3-dihexylthieno[3,4-*b*]pyrazine) film on glass is shown in Figure 2. The spectrum is dominated by the first interband transition with an onset at ≈0.9 eV and a peak at ≈1.3 eV. This observation is in good agreement with the results of Pomerantz et al.[8]

Raman spectroscopy was performed on a Dilor XY spectrometer with a liquid-nitrogen-cooled CCD multichannel detector. For excitation laser lines ranging from 406 nm up to 742 nm from an Ar^+, Kr^+, or Ti:sapphire laser were used. The measurements were taken in backscattering geometry with a laser power below 0.5 mW (70 W/cm^2) and a typical spectral resolution of 4 cm^{-1}. For resonance Raman measurements corrections for spectrometer response and scattering factor are considered. Line positions were obtained from a careful numerical fit using Gaussian and Lorentzian line shapes.

III. Computation Method

The computational work was started by an evaluation of the ground state. For this purpose a method proposed by Karpfen and Kertesz[15] to find the relative stability of the quinonoid (Q) and aromatic (A) forms of the polymer was used. The stabilization energy per repeat unit of the polymer is given by

$$E^N = E_{pru}{}^N(\mathrm{A}) - E_{pru}{}^N(\mathrm{Q}) \qquad (1)$$

where $E_{pru}{}^N = E(N) - E(N-1)$ and $E(N)$ is the total energy of the N-mer in either the Q or A form. Because of the large repeat unit, the calculation was restricted to trimers and dimers. Throughout this study, the *ab initio* software used is Gaussian 92[16] and the basis set is 3-21G.

In order to calculate the polymer vibrational frequencies for each configuration, we used the scaled quantum mechanical oligomer force field (SQMOFF) method which is based on oligomer force fields obtained from *ab initio* calculations.[17,18] in this model the force field for a long-chain polymer having translational symmetry is extracted from an oligomer (trimer). At the 2,3-positions of the polymer, hydrogen replaced the side groups in the calculations. In order to obtain the quinonoid (aromatic) structure, the oligomer was capped with $=CH_2$ (−H) end groups. The former is the Q model, which in the final analysis seems to represent best the average structure of the repeat units of undoped PThP.

In both models the 3-21G basis set was used for structure optimization. The force matrix of the central unit was extracted from the trimer calculation and used for the polymer calculation. Because SCF Hartree–Fock calculations systematically overestimate force constants,[19] it is necessary to scale the force constants of the trimer with a set of empirical scaling factors determined from small molecules. The Pulay scaling scheme[20]

$$F_{i,j}(\mathrm{scaled}) = (S_i F_{i,j}{}^{\mathrm{SCF}} S_j)^{1/2} \qquad (2)$$

was used in this study. The scaling factors of thiophene and pyrazine were obtained by the least-squares fit method using known experimental frequencies. The Pulay scaling scheme requires that internal coordinates be used so that transfer of scaling factors—of similar bond type—is possible between different molecules. Excellent transferability of scaling factors has been demonstrated in previous studies.[18,21,22] This feature is essential for the successful application of the SQMOFF method. In this study, all of the scaling factors were taken from thiophene and pyrazine except the inter-ring scaling factor. This scaling factor was varied manually from 0.80 to 0.50, in decrement of 0.05 initially and then 0.02, to obtain reasonable agreement with the experimental data.

IV. Results

A. Experimental Results. In Figure 3 the Raman spectrum of PThP substituted with R = CH_3 is shown. Two peaks at 1520 and 1560 cm^{-1} are dominant. This spectral region, where usually resonance-enhanced C=C stretching modes are observed, needs a more detailed analysis. As shown in Figure 4 the Raman spectrum between 1400 and 1700 cm^{-1} can be decomposed into various Gaussian lines. In Figure 4a where only one line was used for the structure at around 1560 cm^{-1} the experimental spectrum can be well reproduced by the computer fit except in the region around 1560 cm^{-1}. Therefore, an additional line is used in the numerical line fit in Figure 4b. In this case there is a reasonable good agreement in the whole spectral range between experiment and fit. The fwhm (full width at half-maximum) of the line at 1520 cm^{-1} in both numerical fits is about 25–30 cm^{-1}. In addition to these dominant modes, there are several weaker lines at lower wavenumbers (Figure 3), of which two lines with a Lorent-

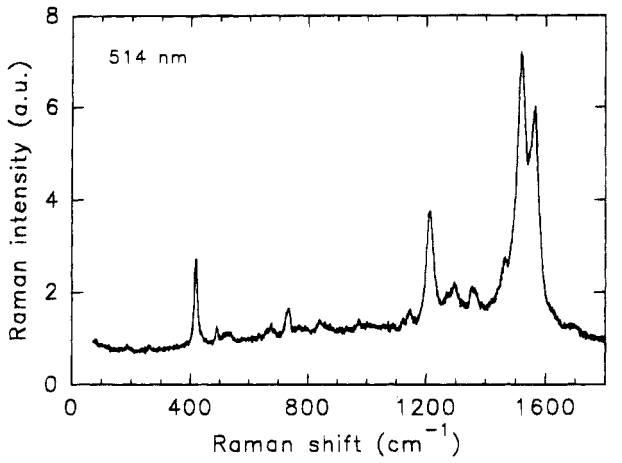

Figure 3. Raman spectrum of poly(2,3-R,R-thieno[3,4-*b*]-pyrazine) with R = CH_3 as excited with 514 nm.

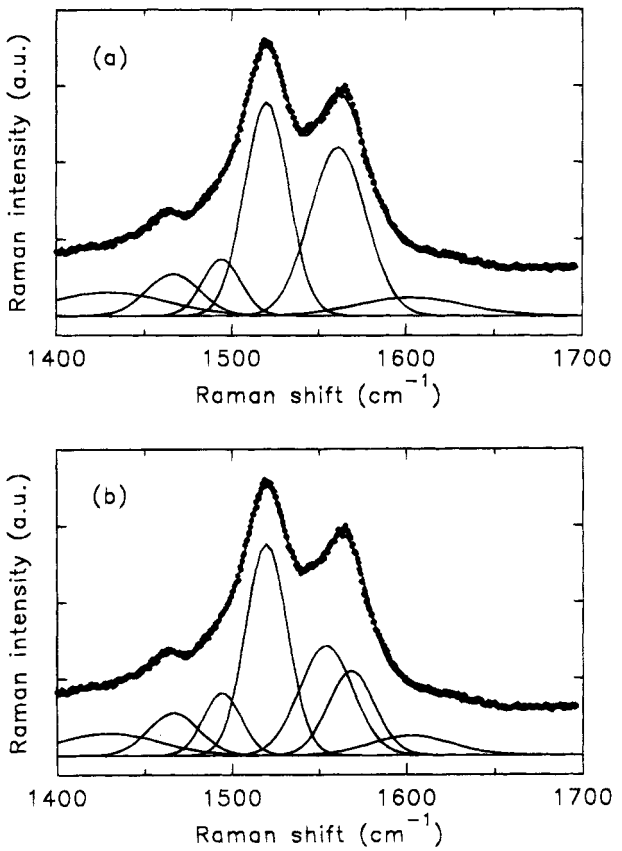

Figure 4. Numerical decomposition of the Raman spectrum of poly(2,3-R,R-thieno[3,4-*b*]pyrazine) with R = CH_3 in various Gaussian lines. The structure at around 1560 cm^{-1} is fitted by one line in a and two lines in b.

zian line shape at about 1210 and 420 cm^{-1} are most prominent.

Polymers substituted with alkyl chains as long as n-$C_{13}H_{27}$ and substituted with thiophene groups were studied. In all cases two peaks at about 1520 and 1560 cm^{-1} dominate the Raman spectrum. However, a slight mode softening with alkyl chain length and a considerable softening for thiophene substitution were observed. The influence of the substituent on the position of the strongest lines is explicitly shown in Figure 5. For simplicity the mean position of the doublet at about 1560 cm^{-1} is plotted. All three features shift to lower wavenumbers with increasing length of the alkyl group. For substitution with thiophene rings these lines are

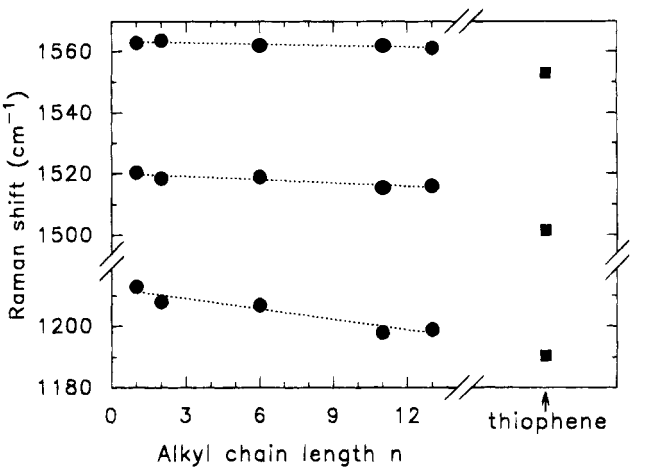

Figure 5. Raman shift of the dominating Raman lines versus alkyl chain length *n* and for the polymer substituted with thiophene rings included on the right side of the figure. For the doublet at around 1560 cm^{-1} the mean position is plotted. The wavelength of the exciting laser was 514 nm.

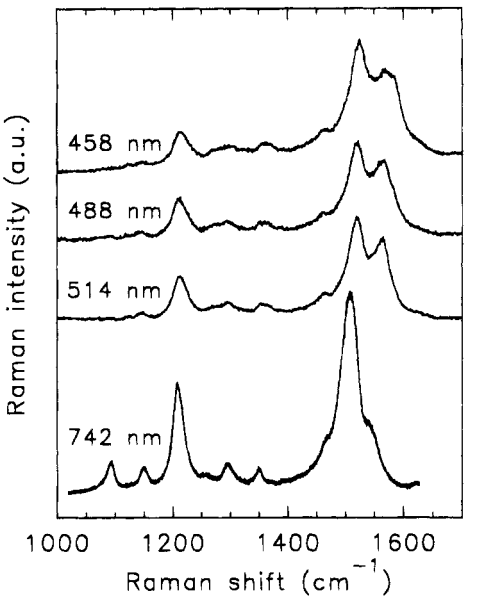

Figure 6. Resonance Raman spectra of poly(2,3-R,R-thieno-[3,4-*b*]pyrazine) with R = CH_3 after excitation with different laser lines as indicated in the figure.

significantly more softened, indicating a change in bonding.

In order to get information about the molecular and electronic structure, the Raman response as a function of the exciting laser energy was studied. Raman spectra of the PThP with R = CH_3 excited with wavelengths ranging from 742 nm down to 458 nm are shown in Figure 6. A line fit analysis revealed that the lines at 1520 cm^{-1} and the doublet at 1560 cm^{-1} shift considerably (1520 cm^{-1}, 16 cm^{-1}/eV; 1560 cm^{-1}, 25 cm^{-1}/eV; when this doublet is fitted with one Gaussian line) and the line at about 1210 cm^{-1} shifts moderately (≈5 cm^{-1}/eV) to lower wavenumbers with increasing wavelength of the exciting laser. This is explicitly depicted in Figure 7, where the Raman shift versus exciting laser energy is plotted. As will be discussed in detail below, this dispersion effect indicates a close relation of these modes to the polymeric backbone. All other lines remain at the same position within a few wavenumbers.

In addition to the line shifts there is also a change in the relative intensities and line widths. For excitation

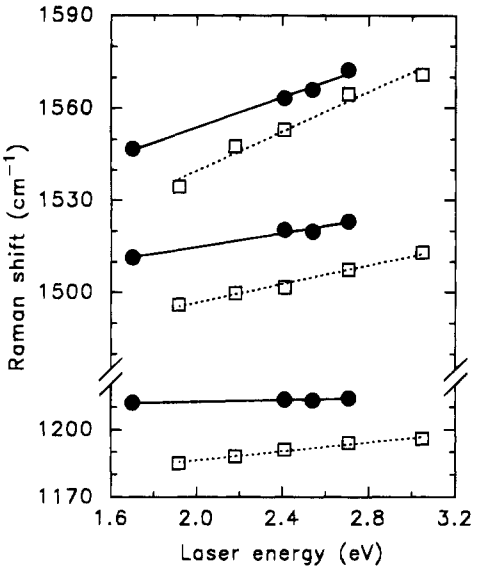

Figure 7. Raman shift of the dominating Raman lines of poly(2,3-R,R-thieno[3,4-*b*]pyrazine) with R = CH_3 (full symbols) and with R = 2-thienyl (open symbols) as a function of the energy of the exciting laser line. For the doublet at 1560 cm^{-1} the mean position is given.

with the red laser (742 nm) the line at 1210 cm^{-1} is strongest and approaches the intensity of the dominant line at 1520 cm^{-1}. In contrast to this behavior, the doublet at 1560 cm^{-1} is weakest as excited with the red laser. Moreover, all lines are narrower as compared to an excitation with a green or blue laser. In order to study the resonance Raman behavior for the various Raman lines, corrections for spectrometer response and scattering factor must be considered. With these corrections the modes at 1091, 1210, and 1520 cm^{-1} decrease with decreasing laser wavelength, whereas the intensities of the strong feature at 1560 cm^{-1} and all other Raman lines remain more or less constant. This indicates differences in electron–phonon coupling.

In Figure 8 resonance Raman spectra for PThP substituted with thiophene groups are shown. Similar to the polymer substituted with CH_3, the strong lines in the region between 1500 and 1600 cm^{-1} exhibit a strong dispersion effect (1500 cm^{-1}, 18 cm^{-1}/eV; 1550 cm^{-1}, 32 cm^{-1}/eV) and the line at about 1210 cm^{-1} a moderate (≈11 cm^{-1}/eV) dispersion effect, whereas all other lines do not shift with the exciting laser energy. According to this result, the dispersion effect is much higher for the thiophene-substituted polymer, as is obvious from the graph in Figure 7. Also the widths of the Raman lines are much larger, indicating more disorder in the thiophene-substituted system. In addition, there is a new line at about 1420 cm^{-1} which is not present in the spectra of alkyl-substituted PThP. This new line is most prominent after excitation with the very blue laser (406 nm).

Doping studies were performed with $FeCl_3$ as a dopant. Figure 9 shows Raman spectra of pristine and $FeCl_3$-doped PThP substituted with R = CH_3 in the spectral region between 1100 and 1700 cm^{-1}. The most striking feature is the intensity change of Raman lines. In the doped polymer the relative intensities of the two strong lines in the C=C stretching region (1520 and 1560 cm^{-1}) change their relative intensities as compared to the pristine polymer. In addition, the line at 1365 cm^{-1} and to a lesser extent also the lines at 1270, 1430, and 1610 cm^{-1} become more intense. A comparison of

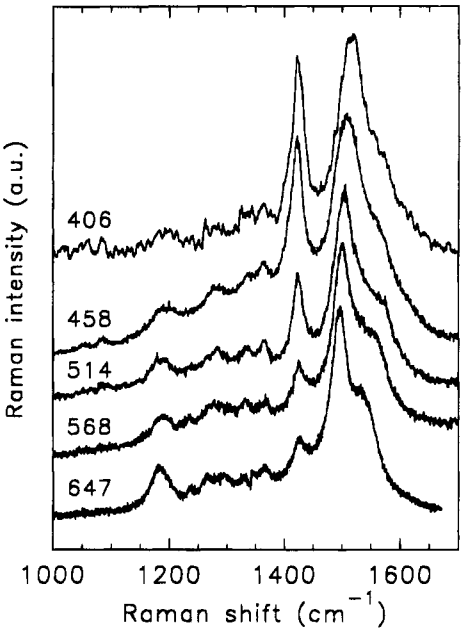

Figure 8. Resonance Raman spectra of poly(2,3-R,R-thieno[3,4-*b*]pyrazine) substituted with thiophene groups after excitation with different laser lines as indicated in the figure. The spectra were normalized to equal intensity of the mode at 1500 cm^{-1}.

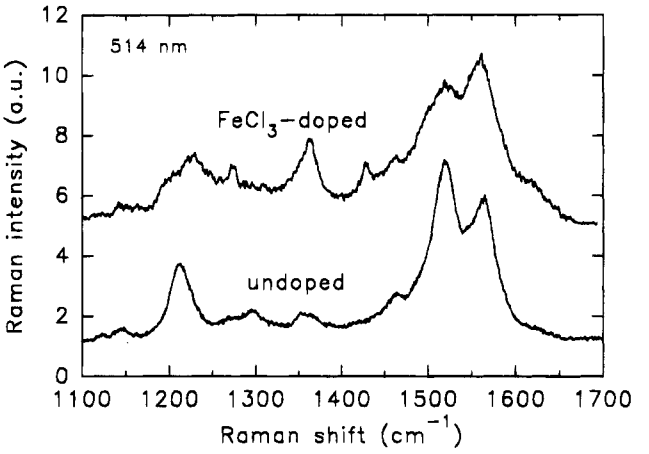

Figure 9. Raman spectra of pristine and $FeCl_3$-doped poly(2,3-R,R-thieno[3,4-*b*]pyrazine) with R = CH_3 as excited with 514 nm.

the Raman modes for the pristine and doped polymer in the spectral region between 1100 and 1700 cm^{-1} is given in Table 1.

B. Theoretical Results. For simplicity and since the vibrational properties will not change much by moderate substitution, we based our theoretical considerations on unsubstituted planar PThP. PThP has the same symmetry as PITN or poly(thiophene) (PT); it belongs to the linear symmetry group $L_{21/mcm}$, which is isomorphous to the point group D_{2h}. Thus, the selection rules are such that IR and Raman activity are mutually exclusive; *gerade* modes are Raman active and *ungerade* modes are IR active. The vibration symmetry analysis yields the following irreducible representation:

$$\Gamma(\mathrm{PThP}) = 11A_g(R) + 5B_{1g}(R) + 11B_{2g}(R) + 5B_{3g}(R) + 5A_u + 10B_{1u} + 5B_{2u} + 10B_{3u} \quad (3)$$

A_g and B_{2g} are in-plane Raman modes, and B_{1g} and B_{3g} are out-of plane Raman modes. Our calculations for the

Table 1. Experimental Values for Raman Mode Frequencies and Intensities for Pristine and $FeCl_3$-Doped Poly(2,3-R,R-thieno[3,4-*b*]pyrazine) (R = CH_3) in the Frequency Region between 1100 and 1700 cm^{-1} as Excited with λ = 514 nm.

position (pristine) (cm^{-1})	intensity[a] (au)	position (doped) (cm^{-1})	intensity (au)
1146	3.6	1148	2
1212	32.2	1223	24
1267	1.8 ↑	1273	6.2
1296	11.6	1296	3
1359	9.6 ↑	1364	28.3
1430	1.2 ↑	1428	10
1466	16.1	1465	17.1
1495	17.6	1497	14.9
1520	100	1518	87
1562	75.8	1562	100
≈1605	10.4	1606	22

[a] The arrows indicate the most pronounced intensity increases from the neutral to the doped polymer.

ground state suggest that the quinonoid form is more stable by about 13 kcal/mol per repeat unit. This energy difference is moderate but significant. On the basis of this result, we used our quinonoid model to study the spectrum of the pristine PThP.

As with the case of doped PPP,[21] an unusually small inter-ring scaling factor (0.55) had to be used in order to obtain reasonable agreement with experimental values. (Usually, the scaling factors obtained at the 3-21G basis set level range from 1.0 to 0.7.) This is primarily due to the overestimation of the double bond character by the Q model. In the Q model, the double bond character of the inter-ring CC bond was ensured by having CH_2 as the terminal group. In the actual polymer, the terminal group is H. Hence, the double bond depicted in the model is stronger than that in the actual polymer. Furthermore, it was shown by Kürti and Surjan[23] that the middle part of a quinonoid PITN chain has the strongest double bond character; there is a gradual decrease in double bond (or increase in single bond) character from the middle to the end of the chain. The overrepresentation of the Q model (in terms of inter-ring CC double bond) and the graduation nature of the double bond character in the actual polymer chain needed an additional correction. Hence, the scaling factor is necessarily lower than the usual value of about 0.75 (for C=C bond). It is also important to note that model Q represented an average structure of the polymer chain.

The inter-ring scaling factor was found to influence mainly the inter-ring mode and to a much lesser extent the weak A_g modes at 1299 and 1360 cm^{-1}. The calculated Raman spectrum of the quinonoid (Q) model together with the experimental spectrum of pristine PThP in the C=C stretching mode region is plotted in Figure 10. Only in-plane modes are observable because all out-of-plane modes have frequencies lower than 1000 cm^{-1}. The experimental and calculated spectra are in good agreement. All major features are reproduced in the latter, including positions and relative intensities. The strongest mode is the inter-ring A_g mode at 1535 cm^{-1}, which is almost at the same position as the strongest mode in the experimental spectrum (1520 cm^{-1}). For comparison experimental and calculated mode frequencies and intensities are summarized in Table 2.

The normal displacement vector diagrams of the two prominent peaks in the 1500–1600 cm^{-1} region are shown in Figure 11. The calculated 1535 cm^{-1} mode is

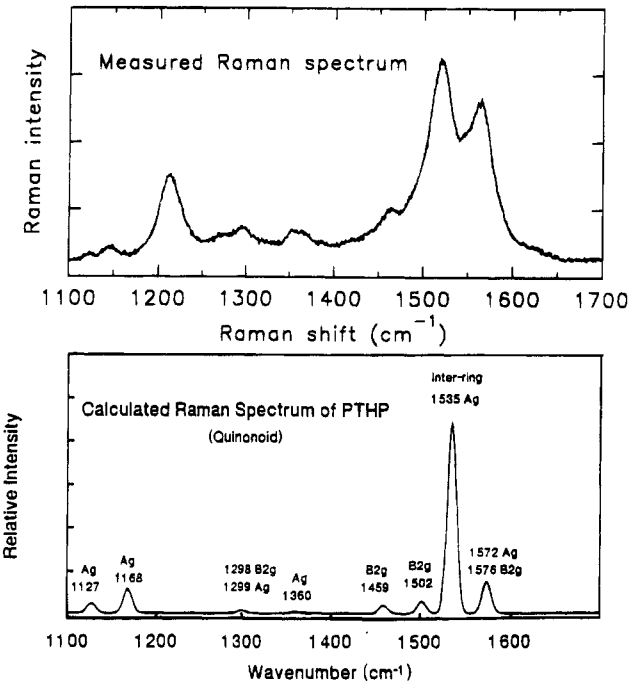

Figure 10. Comparison of the measured (upper curve) Raman spectrum for poly(2,3-R,R-thieno[3,4-*b*]pyrazine) with R = CH_3 and the calculated spectrum (lower curve) for the quinonoid form.

Table 2. Position and Intensity of the Experimentally Observed Raman Modes for Poly(2,3-R,R-thieno[3,4-*b*]pyrazine) (R = CH_3) after Excitation with 514 nm and Calculated Values for the Quinonoid Model of Poly(thieno[3,4-*b*]pyrazine) together with the Assignment

position (exp) (cm^{-1})	intensity (au)	position (calc) (cm^{-1})	intensity (au)	symmetry
259	0.4	241	0.05	A_g
418.5/490	11.6/0.9	464	1.2	A_g
732	6.2	646	0.2	A_g
1008	0.9	1032	0.5	A_g
1146	3.6	1127	4.9	A_g
1212	32.2	1168	13.1	A_g
1267	1.8			
1296	11.6	1298/1299	0.7	B_{2g}/A_g
1359	9.6	1360	0.8	A_g
1430	1.2			
1466	16.1	1459	4.4	B_{2g}
1495	17.6	1502	5.5	B_{2g}
1520	100	1535	100	A_g, inter-ring
1556	42.3	1572	8.6	A_g
1569	28.4	1576	5.9	B_{2g}
≈1605	10.4			
		3060	3.3	A_g

mainly a combination of the C_α–C_β and inter-ring stretching mode. The calculated 1572 cm^{-1} mode comprises mainly intraring stretches.

The aromatic model gives two dominant A_g modes with a strong inter-ring character at 1394 and 1434 cm^{-1} and several weaker A_g and B_{2g} modes. The calculated results for the A_g modes are given in the first two columns of Table 3.

In Figure 12 we show the resultant stretching force constants of the C–C and C–N bonds for quinonoid PThP. In this picture we also compare these values with those of doped poly(thiophene) (PTh),[22] since it has a quinonoid (Q) structure as well, and with undoped PTh which has an aromatic (A) structure. It can be seen that PThP and doped PTh have similar inter-ring stretching force constants. The fusion of a pyrazine ring

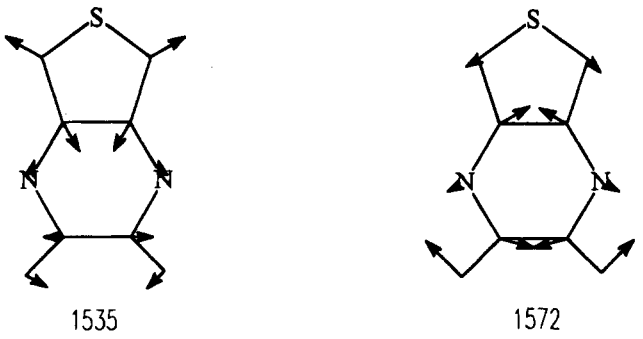

Figure 11. Calculated normal-mode displacement diagrams of the two A_g modes in the 1500–1600 cm^{-1} region.

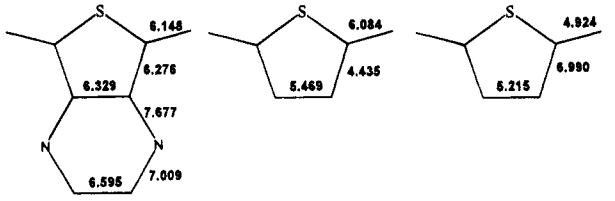

Figure 12. Stretching force constants in mdyn/Å of (from left to right) pristine poly(thienopyrazine) (Q), doped poly(thiophene) (Q), and pristine poly(thiophene) (A).

Table 3. Calculated Values for a_g Raman Mode Frequencies and Intensities for the Aromatic Model of Poly(thieno[3,4-*b*]pyrazine) in Comparison with Experimental Positions for New Raman Modes in these Spectrum of $FeCl_3$-Doped Poly(2,3-R,R-thieno[3,4-*b*]pyrazine) (R = CH_3) after Excitation with λ = 514 nm

position (calc) (cm^{-1})	intensity (au)	position (meas) (cm^{-1})
222	0.01	
480	1.1	
611	1.6	
953	5.4	
1060	0.4	
1203	5.1	
1322	12	1273
1394	100 inter-ring	1364
1434	40.7 inter-ring	1428
1551	0.2	
3030	0.4	

onto the thiophene ring results in the stiffening of both the C_α–C_β and C_β–C_β stretching force constants.

On the basis of the Badger's rule, we fitted the final scaled CC stretching force constants of a number of small molecules vs calculated bond lengths and obtained the relationship to be $F^{-1/3} = 0.63r - 0.35$, where F is the force constant in mdyn/Å and r is the calculated bond length in Å. Hence, the PThP inter-ring CC stretching force constant of 6.148 mdyn/Å can now be estimated to correspond to a bond length of 1.42 Å. Along the line of reasoning given in ref 21 for doped PPP and assuming that "pure aromatic" and "pure quinonoid" CC bond lengths are 1.49 and 1.32 Å, respectively, we conclude that the average inter-ring CC bond length of 1.42 Å corresponds to about 40% quinonoid character.

V. Discussion

A. Effect of Substitution and Resonance Raman Behavior. The basic features of the Raman spectrum for PThP are similar to those of other conjugated polymers like poly(thiophene) or poly(isothianaphthene).[7] It is dominated by lines between 1400 and 1600 cm^{-1} originating from C=C stretching modes. Due to a strong electron–phonon coupling, these modes are resonance enhanced probably by the HOMO–LUMO (highest occupied molecular orbital–lowest unoccupied molecular orbital) electronic transition. The widths of the two dominant Raman features at 1520 and 1560 cm^{-1} are comparable to the values reported for other conjugated polymers.[7,9] However, despite the strong resemblance in molecular structure, the spectrum of PThP is much simpler as that of PITN.[3,5] For PITN Raman lines for various short oligomers (n = 3–7) were found in the spectrum since its effective conjugation length was assumed to be very small.[3,5] In contrast to that the conjugation length of PThP seems to be considerably higher since no particular lines originating from oligomers are evident in the Raman spectra.

Similar to alkyl-substituted poly(thiophene),[24] the introduction of long alkyl side chains in the molecular structure of PThP leads to a considerable increase in solubility and thus to an improvement in processability. The electronic structure is, on the other hand, only slightly affected, as can be seen from the rather minor changes in the Raman spectrum. Only for some modes a very moderate shift to lower wavenumbers with increasing alkyl chain length was observed. This small effect can be attributed, on the one hand, to slight changes in the electronic structure in the vicinity of the substituent and, on the other hand, to changes in the conjugation length. An increase in conjugation length due to a stabilization effect by the side chains might account for the observed mode softening. The considerable change in the Raman line positions observed for the thiophene-substituted PThP suggests a different situation. This is not surprising because of the strong chromophoric character of the π-electrons in the thiophene ring which leads to a change of π-electron density along the polymeric backbone and thus to a change in force constants and mode frequencies. Moreover, the increased line widths indicate more disorder in the system as compared to alkyl-substituted PThP.

As in other conjugated polymers, some Raman lines for PThP exhibit a dispersion effect, while others do not. The strongly resonance-enhanced Raman lines shift with the energy of the exciting laser line. This effect is moderate for the line at 1210 cm^{-1} and higher for the 1520 cm^{-1} line and for the doublet at 1560 cm^{-1}. It originates from the correlation between the order and electronic structure.[7,25,26] The conjugation along the chain is considered to be interrupted by defects and thus extends only to a finite length. Since both the electronic transition energies and the force constants of the system depend on the length of the conjugated segments, a photoselective resonance excitation occurs in the Raman process. A superposition from all segments gives the observed Raman line for all laser excitations. A quantitative description of the dispersion phenomenon is given by the conjugation length theory.[25,26] This model can be applied to the results presented here. It is straightforward to understand that a bond which is far enough displaced from the backbone will not suffer from any change in the conjugation length. A good example is the dispersionless Raman line at 1420 cm^{-1} in the thiophene-substituted PThP. From its dispersionless character it can be assigned safely to the substituted thiophene rings. The strong dispersion observed for the lines at 1520 and 1560 cm^{-1} suggests, on the other hand, that these modes originate from bonds closer to the backbone.

Another conclusion can be drawn from the difference in dispersion of alkyl- and thiophene-substituted PThP, since the extent of line shift with laser energy is also a measure for disorder and conjugation length. The higher dispersion effect for thiophene substitution is an indication for a lower conjugation length and more defects in this system, which is consistent with the larger widths of the lines.

The additional line for thiophene-substituted PThP at 1420 cm^{-1} has a very different resonance Raman behavior as compared to the other lines. Its relative intensity is highest for excitation with the blue laser. This is another strong indication that this line originates from the thiophene substituents, which are only weakly correlated to the polymer backbone.

B. Ground-State Geometry and Assignment of the Vibrational Modes. As calculated the quinonoid structure is by 13 kcal/mol per repeat unit more stable than the aromatic form. This value is higher than the stabilization energy for the quinonoid form of PITN, which is only 2.4 kcal/mol per repeat unit.[10] The quinonoid ground-state geometry obtained here is consistent with results of Nayak and Marynick[13] obtained by using the PRDDO method.

The fusion of a pyrazine onto the thiophene ring in PThP has important consequences to the molecular and electronic structure. As is shown in section IV.B, it leads to a stiffening of both the $C_\alpha-C_\beta$ and $C_\beta-C_\beta$ stretching force constants (see Figure 12). Therefore, the inter-ring stretching frequency of PThP is higher as compared to that of doped PTh (1418 cm^{-1})[27,28] due to the increase in these CC stretching force constants which are coupled to the inter-ring stretching modes (see Figure 11). This change in bonding and force constants leads to a considerable decrease in bond length alternation. As can be seen in Figure 11, the force constants along the polymeric backbone change only by a few percent. According to the theoretical results of Bredas et al.,[2] this decrease in alternation is responsible for the very low band gap of 0.9 eV for PThP.

It is well-known that *ab initio* calculations, when used in conjunction with appropriate force constant scaling, can reproduce well the experimental frequencies and give reasonable intensities.[17,18] For a correct vibrational analysis the experimentally observed Raman lines must agree well in position and intensity with the calculations, but also the nature of the vibrations given by the displacement vectors can be very helpful. Before discussing all modes we start with the most pronounced feature. We assign the strongest mode in the experimental spectrum at 1520 cm^{-1} to the calculated inter-ring mode at 1535 cm^{-1}. This is based on the following arguments:

1. The measured frequency (1520 cm^{-1}) agrees well with the calculated frequency (1535 cm^{-1}).

2. The line at 1520 cm^{-1} in the measured spectrum as well as the calculated inter-ring mode is strongest in the spectra. The dominance of the line at 1520 cm^{-1} in the experimental spectrum is most pronounced after excitation with the red laser.

3. The line at 1520 cm^{-1} exhibits a strong dispersion as one would expect for the inter-ring mode.

4. The resonance Raman behavior of the line at 1520 cm^{-1} shows a strong coupling to the HOMO–LUMO electronic transition, indicating a close relation to the polymeric backbone.

After identification of the inter-ring mode all other observed Raman lines can be assigned to A_g and B_{2g} modes as given in Table 2. The modes at 1210 and 1520 cm^{-1} are strongest and A_g. The double peak structure at 1560 cm^{-1} is a superposition of an A_g mode and a B_{2g} mode. There is a surprisingly good agreement between theoretical and experimental results. However, from the calculations the inter-ring characteristics of the A_g mode at 1572 cm^{-1} is very low (less than 2%) although the observed strong shift of the mean position for the doublet at 1560 cm^{-1} with the energy of the exciting laser indicates at a first glance a close relation to the polymeric backbone. It should be kept in mind, however, that the dispersion of the two individual lines at 1560 cm^{-1} (A_g and B_{2g} mode) can be much lower than the shift of the mean position. The two lines might change their relative intensities with the energy of the exciting laser and pretend in this way a strong dispersion, although the individual lines shift only slightly. This idea was proven by a careful numerical line fit. In the described way a dispersion of about 7–10 cm^{-1}/eV was obtained for both lines of the doublet at 1560 cm^{-1}, which is considerably lower than the value (16 cm^{-1}/eV) measured for the Raman line at 1520 cm^{-1}.

Doping of a quinonoid polymer leads, in general, to an aromatic structure. However, one has to keep in mind that a complete transformation occurs only for a fully doped state. In a realistic system contributions from both doped and neutral segments of the polymer will always appear in the Raman spectrum, as, for example, in the case of poly(acetylene) or poly(thiophene).[28] In the spectrum of $FeCl_3$-doped PThP several additional features appear. We assign these new lines to modes of the doped polymer which corresponds to aromatic segments. They are compared with theoretical results for the aromatic form of PThP in Table 3. At least for the strongest calculated modes (1322, 1394, and 1434 cm^{-1}) good agreement with the additionally observed Raman lines is obtained. These results confirm the aromatic structure for doped PThP and the quinonoid ground state for the neutral polymer.

VI. Conclusion

We have presented a vibrational analysis of poly(thieno[3,4-*b*]pyrazine) and various derivatives by resonance Raman scattering and theoretical calculations for the mode frequencies of the quinonoid and aromatic forms of PThP.

Various compounds substituted with alkyl side groups as long as n-$C_{13}H_{27}$ and thiophene groups have been prepared and characterized. The Raman spectra of all materials studied are dominated by two structures at about 1520 and 1560 cm^{-1}. They were assigned to the inter-ring A_g vibration and to a superposition of an A_g and B_{2g} mode. These lines exhibit a dispersion effect with the energy of the exciting laser. Alkyl substitution has only a minor influence on the electronic structure, whereas substitution with thiophene groups leads to a change of π-electron density along the polymeric backbone and to a considerable mode softening. In addition, thiophene substitution induces some disorder, which is reflected by a line broadening and an increase in dispersion. Doping with $FeCl_3$ results in slight line shifts and in significant relative intensity changes. From energetics calculations and from a comparison of the experimental and theoretical vibrational results, we have shown that the ground-state geometry of PThP is quinonoid in the neutral state and aromatic in the doped state.

Acknowledgment. This work was supported by the FFWF Project P7506-TEC, BMfWF Project GZ 45.338/1-IV/6a/94, NSF Grant DMR-91-15548, and the Pittsburgh Supercomputer Center Grant DMR-920006P.

References and Notes

(1) Wudl, F.; Kobayashi, M.; Heeger, A. J. *J. Org. Chem.* **1984**, *49*, 3382.
(2) (a) Bredas, J. L.; Heeger, A. J.; Wudl, F. *J. Chem. Phys.* **1986**, *85*, 4673. (b) Bredas, J. L. *J. Chem. Phys.* **1985**, *82*, 3808.
(3) Cuff, L.; Kertesz, M.; Geisselbrecht, J.; Kürti, J.; Kuzmany, H. *Synth. Met.* **1993**, *55–57*, 564.
(4) (a) Hanack, M.; Mangold, K.-M.; Röhring, U.; Maichle-Mössner, C. *Synth. Met.* **1993**, *60*, 199. (b) Lakshmikanthan, M. V.; Loraj, D.; Scordilis-Kelley, C.; Wu, X.-L.; Prakka, J. P.; Metzger, R. M.; Cava, M. P. *Adv. Mater.* **1993**, *5*, 723. (c) Musmanni, S.; Ferraris, J. P. *J. Chem. Soc., Chem. Commun.* **1993**, 172.
(5) Wallnöffer, W.; Faulques, E.; Kuzmany, H.; Eichinger, K. *Synth. Met.* **1989**, *28*, C533.
(6) Kürti, J.; Surjan, P. R.; Kertesz, M. *J. Am. Chem. Soc.* **1991**, *113*, 9865.
(7) Kuzmany, H.; Kastner, J. In *Macromolecules 1992*; Kahovec, J., Ed.; VSP: Zeist, The Netherlands, 1993; p 333.
(8) Pomerantz, M.; Chaloner-Gill, B.; Harding, L. O.; Tseng, J. J.; Pomerantz, W. J. *J. Chem. Soc., Chem. Commun.* **1992**, 16721.
(9) Kastner, J.; Kuzmany, H.; Curran, S.; Davey, S.; Blau, W.; Bräunling, H. *Condens. Matter Mater. Commun.* **1994**, *1*, 812.
(10) (a) Lee, Y. S.; Kertesz, M. *J. Chem. Phys.* **1988**, *88*, 2609. (b) Lee, Y. S.; Kertesz, M. *Int. J. Quantum Chem., Quantum Chem. Symp.* **1987**, *21*, 163.
(11) Hoogmartens, I.; Adriaensen, P.; Vanderzande, D.; Gelan, J.; Quattrocchi, C.; Lazzaroni, R.; Bredas, J. L. *Macromolecules* **1992**, *25*, 7347.
(12) (a) Magnoni, C.; Zerbi, G. Proceedings of the International Conference on Science and Technology of Synthetic Metals, 1994, Seoul, Korea, *Synth. Met.*, in press. (b) Quattrocchi, C.; Lazzaroni, R.; Bredas, J. L.; Kiebooms, R.; Vanderzande, D.; Gelan, J. Proceedings of the International Conference on Science and Technology of Synthetic Metals, 1994, Seoul, Korea, *Synth. Met.*, in press.
(13) Nayak, K.; Marynick, D. S. *Macromolecules* **1990**, *23*, 2237.
(14) (a) Vegh, D.; Landl, M.; Kastner, J.; Kuzmany, H. *Synth. Commun.*, in press. (b) Kastner, J.; Kuzmany, H.; Vegh, D.; Landl, M.; Cuff, L.; Kertesz, M. Proceedings of the International Conference on Science and Technology of Synthetic Metals, 1994, Seoul, Korea, *Synth. Met.*, in press.
(15) Karpfen, A.; Kertesz, M. *J. Phys. Chem.* **1991**, *95*, 7680.
(16) Frisch, M. J.; Head-Gordon, M.; Trucks, G. W.; Gill, P. M. W.; Wong, M. W.; Foresman, J. B.; Johnson, B. G.; Schlegel, H. B.; Robb, M. A.; Replogle, E. S.; Gomperts, R.; Andres, J. L.; Raghavachari, K.; Binkley, J. S.; Gonzalez, C.; Martin, R. L.; Fox, D. J.; Defrees, D. J.; Baker, J.; Stewart, J. J. P.; Pople, J. Gaussian Inc., Pittsburgh, 1992.
(17) Cui, C. X.; Kertesz, M. *J. Chem. Phys.* **1990**, *93*, 5257.
(18) Cuff, L.; Kertesz, M. *Macromolecules* **1994**, *27*, 762.
(19) Pople, J. A.; Schlegel, H. B.; Krishnan, R.; Defrees, D. J.; Binkley, J. S.; Frisch, M. J.; White, R. A.; Hout, R. F.; Hehre, W. J. *Int. J. Quantum Chem., Quantum Chem. Symp.* **1981**, *15*, 267.
(20) Pulay, P.; Fogarasi, G.; Boggs, J. E.; Vargha, A. *J. Am. Chem. Soc.* **1983**, *105*, 7037.
(21) Cuff, L.; Cui, C.; Kertesz, M. *J. Am. Chem. Soc.* **1994**, *116*, 9269.
(22) Cuff, L.; Kertesz, M. *J. Phys. Chem.* **1994**, *98*, 12223.
(23) Kürti, J.; Surjan, P. R. *J. Chem. Phys.* **1994**, *92*, 3247.
(24) Danno, T.; Kürti, J.; Kuzmany, H. *Phys. Rev.* **1991**, *B43*, 4809.
(25) Kuzmany, H. *Phys. Stat. Solidi* **1980**, *B97*, 521.
(26) (a) Kastner, J.; Kuzmany, H.; Paloheimo, J.; Dyreklev, P. *Synth. Met.* **1993**, *55–57*, 558. (b) Kastner, J.; Pichler, T.; Kuzmany, H.; Curran, S.; Blau, W.; Weldon, D. N.; Delamesiere, M.; Draper, S.; Zandbergen, H. *Chem. Phys. Lett.* **1994**, *221*, 53. (c) Kastner, J.; Kuzmany, H.; Dousek, F. P.; Kavan, L.; Kürti, J. *Macromolecules* **1995**, *28*, 344.
(27) Louarn, G.; Mevellec, J. Y.; Buisson, J. P.; Lefrant, S. *J. Chem. Phys.* **1992**, *89*, 987.
(28) Danno, T.; Kastner, J.; Kuzmany, H. *Synth. Met.* **1993**, *58*, 257.

MA946037J